J Electroceram (2010) 25:20–25
DOI 10.1007/s10832-009-9584-9

Effect of excess PbO on microstructure and orientation of PZT(60/40) films

Chee-Sung Park · Jae-Wung Lee · Sung-Mi Lee · Shin-Hee Jun · Hyoun-Ee Kim

Received: 5 January 2009 / Accepted: 23 June 2009 / Published online: 7 July 2009

Abstract Lead zirconate titanate [PZT(60/40)] films were deposited by RF-magnetron sputtering using single oxide targets with various levels of excess PbO. The excess PbO in the film played an important role in the pyrochlore-to-perovskite transformation, nucleation and growth processes, orientation control, and crack formation. When 5% or 20% excess PbO was added to the target, pyrochlore phases were created and the films were severely cracked. However, the films had a perovskite structure without any pyrochlore phases when 10% or 15% excess PbO was added to the targets. More interestingly, the crystallographic orientation was strongly dependant on the excess PbO content. A film with a (111) preferred orientation was produced when 10% excess PbO was added to the target. On the other hand, a film with a (100) preferred orientation was deposited by the target with 15% excess PbO. The dielectric, ferroelectric and piezoelectric properties of these films with different orientations and microstructures were examined and correlated with the film structure.

Keywords PZT film · Piezoelectric · Microstructure

1 Introduction

Lead zirconate titanate (PZT) films have attracted considerable attention for their potential use in nonvolatile ferroelectric random access memories (FeRAM) as well as in microelectromechanical systems (MEMS) [1-4]. The strong piezoelectric response of PZT films makes electromechanical sensing and actuation possible.

High quality PZT films have been fabricated using a variety of chemical and physical deposition methods including sputtering, pulsed laser deposition (PLD), metal organic chemical vapor deposition (MOCVD) and sol-gel method. Regardless of the deposition method, excess PbO is usually added to the specimen to compensate for the loss of Pb caused by its volatilization as well as to achieve film stoichiometry [5, 6]. Therefore, one of the primary factors in the synthesis and crystallization of PZT films is the proper control of the Pb content in order to acquire high quality and reproducible films.

The crystallographic orientation of the PZT film is one of the most important factors that determine its electrical properties [7, 8]. The nucleation and growth stage is a critical step for determining the preferred orientation [9-12]. There have been several studies that examined why PZT films have a preferred orientation on a platinized silicon substrate. The nucleation and growth kinetics can be controlled by a lattice matching mechanism guided by an intermediate phase or energetically stable nuclei [9-12].

Regarding the nucleation and growth mechanism, the behavior of Pb in a PZT film is important for determining its structural properties. The orientation of a film deposited using the sol-gel method with organics is influenced more strongly by the pyrolysis process than by the amount of excess Pb; therefore, the combustion characteristics (thermal stability and organic contents) determine the behavior of Pb during pyrolysis [6, 9-11, 13]. On the other hand, the films deposited by sputtering do not require a pyrolysis step. Therefore, the Pb content in the film is a more important factor for determining the nucleation and growth process [12]. In this study, we investigated the effect of excess PbO in the PZT films deposited by changing the Pb

C.-S. Park · J.-W. Lee · S.-M. Lee · S.-H. Jun · H.-E. Kim (✉)
Department of Materials Science and Engineering and Research Institute of Advanced Materials (RIAM),
Seoul National University,
Seoul 151-744, Korea
e-mail: kimhe@snu.ac.kr

content in the targets without organics. The microstructural evolution and electrical properties were investigated.

2 Experimental procedure

A rhombohedral composition [PZT(60/40)] was selected due to the fact that the oriented rhombohedral films near the morphotropic phase boundary (MPB) are expected to have excellent electrical properties [7, 8, 14]. PZT(60/40) films with various Pb contents were deposited by RF magnetron sputtering. Single oxide targets were prepared using a conventional mixed oxide method with a composition of $Pb_{1+\alpha}(Zr_{0.6}Ti_{0.4})O_3$ (α varying from 0.05 to 0.2). Pure PbO, ZrO_2, and TiO_2 powders (all 99.9% purity, Aldrich, Milwaukee, WI, USA) were weighed and mixed by ball-milling with zirconia balls as media in alcohol. After mixing and drying, the mixture was calcined in a covered alumina crucible at 800°C for 2 h. The calcined powders were ball-milled again for 24 h. After drying and sieving, the powders were pressed with a 4-inch-diameter mold, followed by cold isostatic pressing again at 300 MPa. The specimens were sintered at 1200°C for 2 h in a double-sealed alumina crucible. Finally, the targets were machined to a diameter of 3 inches.

The PZT films were deposited by sputtering using the abovementioned targets. The deposition conditions are described in [14]. During the sputtering process, the substrate was not heated intentionally; but the substrate temperature increased gradually to 140°C due to an ion bombardment effect. Annealing was carried out at 650°C for 15 min in air with a heating rate of approximately 60°C/min.

X-ray diffraction (XRD; θ–2θ scanning, M18XHF-SRA, Mac Science, Yokohama, Japan) was used to monitor the orientation of the films. The microstructure and thickness of the films were determined by field-emission scanning electron microscopy (FE-SEM; JSM-6330F, JEOL, Tokyo, Japan). Electron probe X-ray micro analysis (EPMA; JXA-8900R, JEOL, Tokyo, Japan) was used to examine the compositions of the as-deposited films. The residual stress was determined by high resolution XRD (HRXRD; X'pert PRO, PANanlytical, Almelo, Netherlands). The ferroelectric properties were measured using a thin film analyzer (TF-analyzer 2000, AixACCT Technologies, Aachen, Germany). The dielectric properties were monitored using an LCR meter (Agilent 4284A, Agilent Technologies, CA, USA) and the pneumatic loading method (PLM) was used to estimate the piezoelectric coefficients [15].

3 Results and discussion

Figure 1 shows the microstructures of the PZT films as a function of the amount of excess PbO deposited on the platinized silicon substrate. The film deposited by the target with 5% excess PbO contained cracks, as shown in Fig. 1 (a). The cross-sectional image of the film also shows relatively large grains as shown in Fig. 1 (b). A magnified view of Fig. 1 (b) shows nano-size particles that were deemed to be a pyrochlore phase. On the other hand, there were no cracks in the films when 10% or 15% excess PbO was added to the targets [Figs. 1 (c–f)]. The film deposited from the target with 10% excess PbO contained large in-plain grains (1.9 μm) with an equiaxed columnar structure, as shown in Figs. 1 (c, d). On the other hand, the film deposited from the target with 15% excess of PbO showed small in-plain grains (~ 0.2 μm) with a fine columnar structure, as shown in Figs. 1 (e, f). The film deposited from the target with 20% excess PbO showed severe cracking, as shown in Figs. 1 (g, h). Moreover, the presence of condensed PbO on its surface [Fig. 1 (g)] indicates that the film contained too much PbO, and the grains were quite large. As a result, it was found that cracks are easily generated in the films with a pyrochlore phase, mixed and random orientation, and non-columnar structure, while those with a preferred orientation and columnar structure are resistant to crack formation.

Figures 2 (a–d) shows XRD patterns of the PZT film deposited on the $Pt(111)/Ti/SiO_2/Si$ substrate using targets with different amounts of excess PbO. When 5% excess of PbO was added to the target, the film had a mixed orientation and a Pb-deficient pyrochlore phase [$Pb_2(Zr, Ti)_3O_7$], [11, 16, 17] as shown in Fig. 2 (a). This broad peak of the pyrochlore phase indicates that it is composed of very small crystals, as shown in Fig. 1 (b). However, when 10% excess of PbO was added to the targets, the films showed the (111) preferred orientation without any pyrochlore phase, as shown in Fig. 2 (b). The films had the (100) preferred orientation when 15% excess of PbO was added to the target, as shown in Fig. 2 (c). On the other hand, the film was randomly oriented when 20% excess of PbO was added to the target, as shown in Fig. 2 (d). The orientation and pyrochlore-to-perovskite transformation of the films were strongly influenced by the amount of excess PbO in the targets. These results suggest that the PbO content in the films plays an important role in the nucleation and growth processes in the films during annealing. Moreover, the films with the (111) or (100) preferred orientation were resulted in heterogeneous nucleation and growth, while homogeneous nucleation and growth occurred for those with a randomized orientation.

The compositions of the as-deposited and annealed films were analyzed by EPMA, as shown in Fig. 3. The Pb content in the films increased with increasing excess Pb content in the targets, as expected. However, the amount of Pb in the as-deposited films was higher than that in the targets. The Pb content in the films was reduced markedly

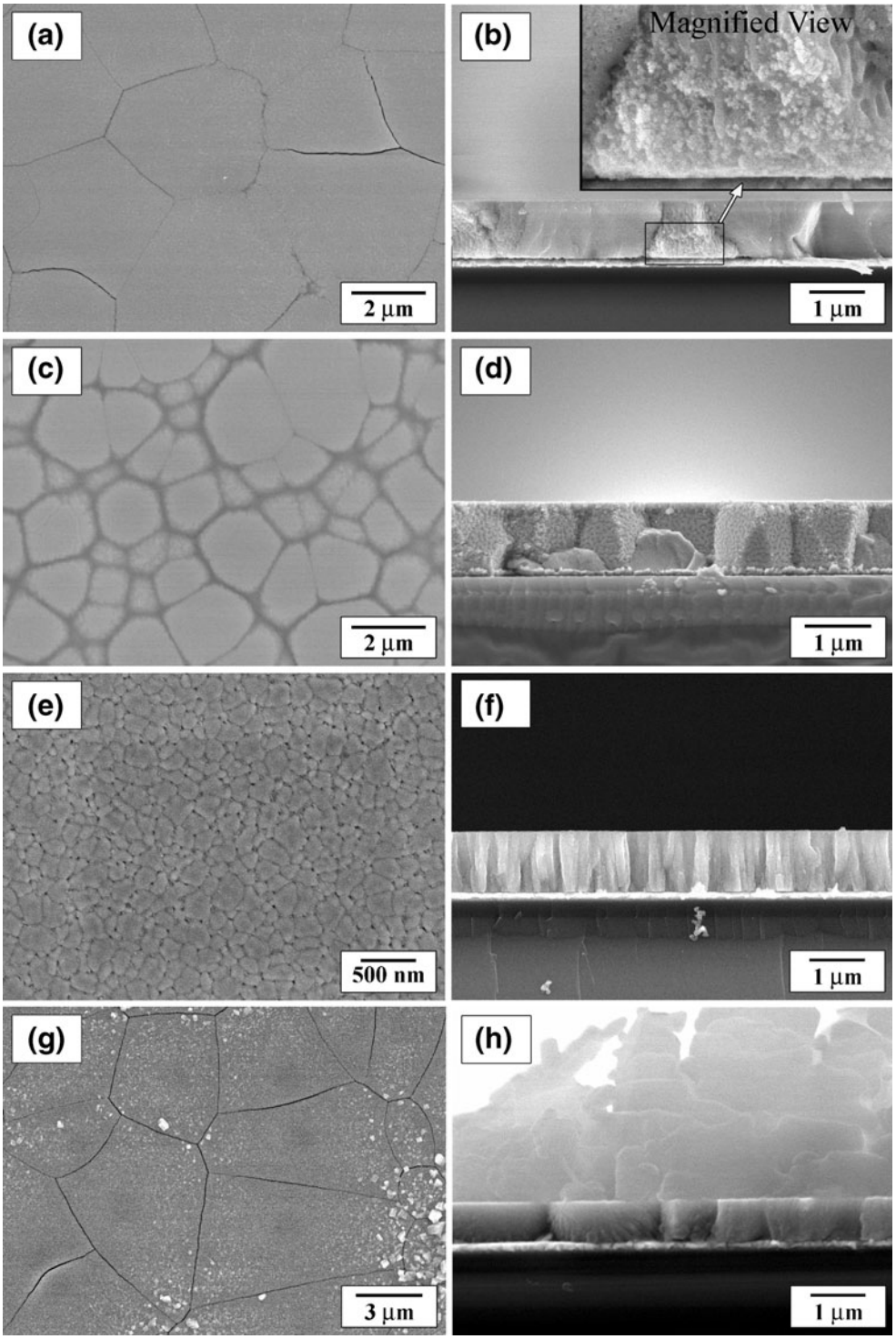

Fig. 1 SEM micrographs of the PZT films deposited using PZT (60/40) targets with different amounts of excess PbO; (**a**) and (**b**) 5 mole%, (**c**) and (**d**) 10 mole %, (**e**) and (**f**) 15 mole %, (**g**) and (**f**) 20 mole %. All the films were annealed at 650°C for 15 min

after annealing [Fig. 3 (a)]. In particular, the annealed film deposited from the target with 10 mole % excess PbO was almost stoichiometric. On the other hand, the Zr/Ti ratio was almost constant (near 60/40) regardless of the amount of excess PbO in the target, as shown in Fig. 3 (b). Therefore, the Pb content in the as-deposited films is proportional to the Pb content in the target, while their Zr and Ti contents remain unchanged. Moreover, approximately 10 mole % of the PbO in the films volatilized during the annealing process to form the perovskite phase. These results indicate that the amount of the PbO in the film strongly influences the nucleation and growth processes; consequently, the microstructural properties are determined by it.

The generation of cracks was correlated to the microstructure and orientation of the film affected by the PbO content. The film deposited from the target with 5% excess

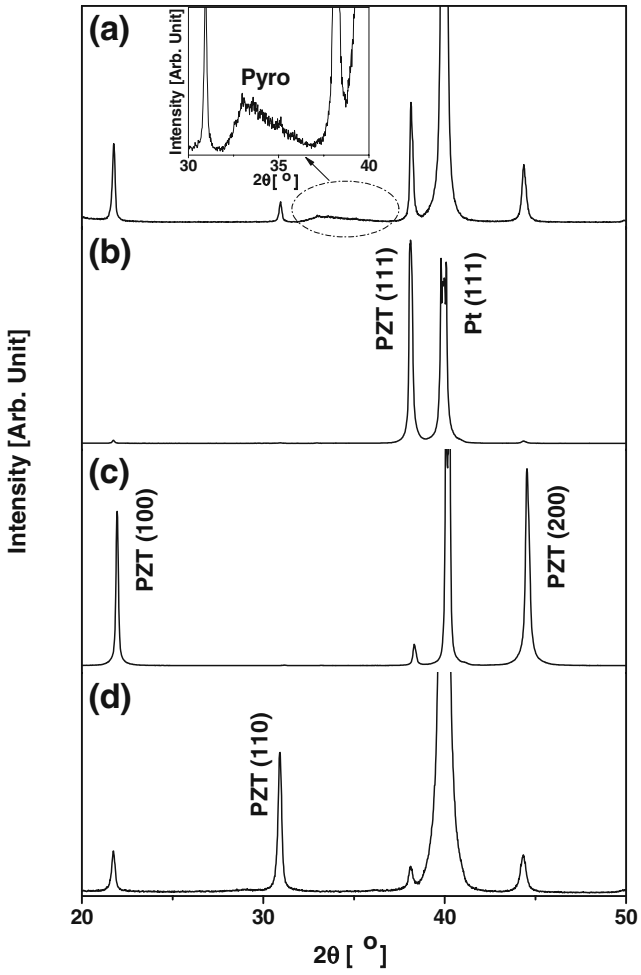

Fig. 2 XRD patterns of the PZT films deposited on a Pt(111)/Ti/SiO_2/Si substrate. (**a**), (**b**), (**c**), and (**d**) were deposited using PZT(60/40) targets containing excess PbO of 5, 10, 15, and 20 mole % of excess PbO, respectively

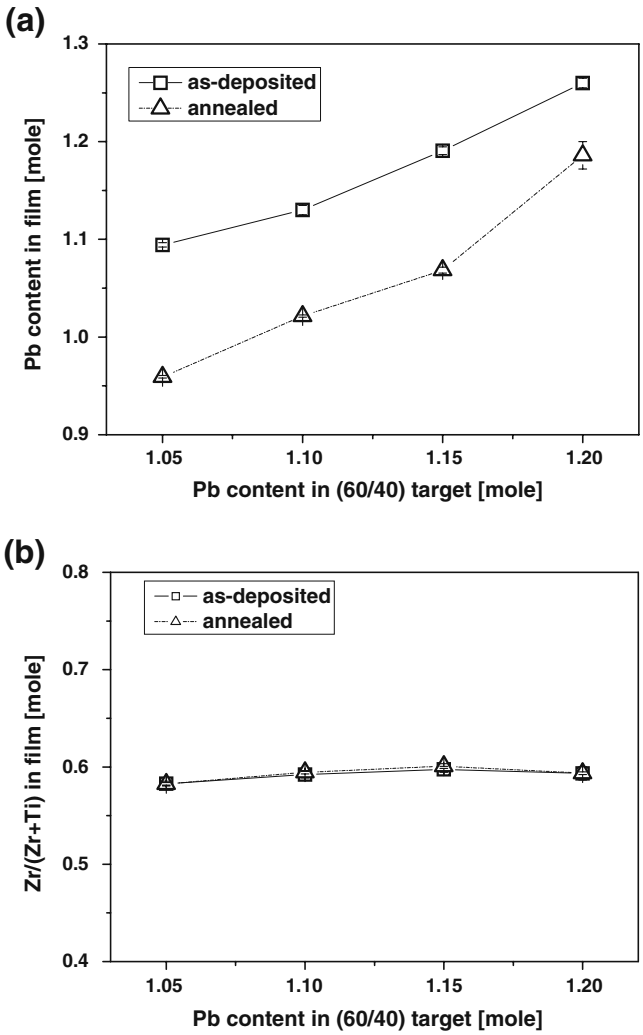

Fig. 3 Composition of the as-deposited and annealed films according to EPMA; (**a**) Pb, (**b**) Zr/Ti ratio

PbO contained a relatively lower amount of PbO, which led to an insufficient pyrochlore-to-perovskite transformation during the annealing process. The film contained a Pb-deficient pyrochlore phase, a mixed orientation, and large grains with cracks. The film deposited using the target with 10% excess PbO contained a suitable amount of excess Pb, which led to stoichiometry and a (111) preferred orientation without any pyrochlore phases. The film had a (111) orientation and a coarse columnar structure without any cracks. The film deposited from the target with 15% excess PbO contained a suitable amount of excess Pb, which led to a (100) preferred orientation. The film grew heterogeneously with a (100) orientation and had a fine columnar structure without cracks. The film deposited from the target with 20% excess PbO contained too much PbO, which led to a random orientation. The film showed a random orientation, exaggerated grains, condensed PbO crystals, and severe cracks. The generation of cracks was attributed to the excessively large grain size and mismatch of the grains.

The electrical properties of the crack-free films produced by the targets containing 10 and 15% excess PbO were analyzed. Figure 4 shows the polarization behavior of the (100) and (111) oriented films as a function of the electric field. The (100) oriented film (15% excess PbO in the target) showed a lower remanant polarization (P_r) and coercive field (E_c). On the other hand, the (111) film (10% excess PbO in the target) had higher P_r and E_c values. Consequently, the shape of the hysteresis loop in the (111) film became more square-like, while that in the (100) was shallow.

Figure 5 shows the dielectric constant and loss of the (100) and (111) oriented films. The dielectric constant of the (100) film was 3 times higher than that of the (111) film, while the dielectric loss of the (100) film was similar to that of the (111) film. As a result, the (100) oriented film has higher dielectric properties than the (111) oriented film. It is well known that (100) oriented films have higher dielectric and piezoelectric properties [7, 8, 13, 14].

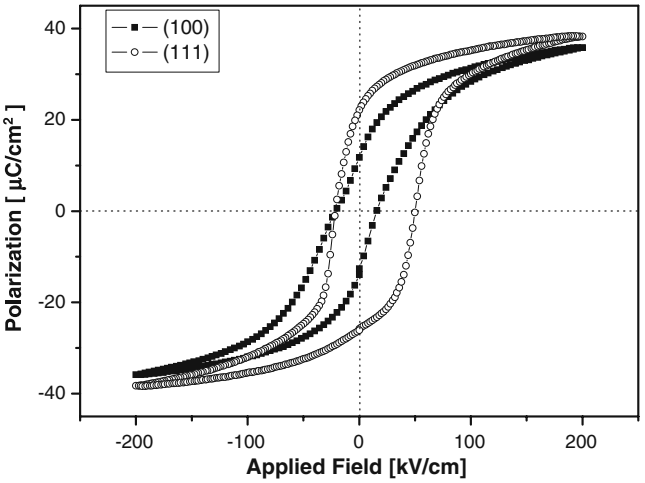

Fig. 4 P-E curves of the (100) and (111) oriented films

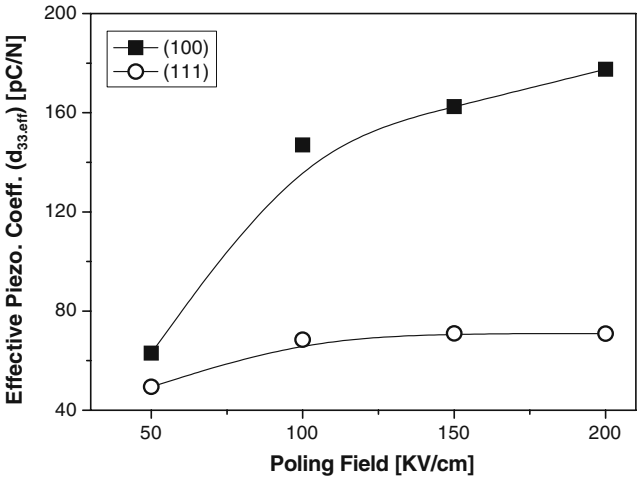

Fig. 6 Piezoelectric properties of the (100) and (111) oriented films as a function of the poling field

Figure 6 shows the effective d_{33} values of the (100) and (111) films measured using the pneumatic load method (PLM), [15] as a function of the poling field. As the poling field increased, the effective d_{33} value in the (111) films increased slightly, whereas it increased to a much greater extent in the (100) films. In particular, the d_{33} value of the (100) and (111) films was 178 pC/N, and 71 pC/N, respectively, when the films were poled at 200 kV/cm.

The electrical properties of these two types of films were caused by their different orientation and microstructural characteristics which were derived from the change in the PbO content. The electrical properties of the films strongly depend on their crystallographic orientations [7, 8, 13, 14]. Moreover, the residual stress derived from the decrease in the grain size can also affect their dielectric and piezoelectric properties [18, 19]. The residual stresses of the films without cracks, but with different orientations and grain sizes, were measured by HRXRD using the $\sin^2\psi$ method. The results are shown in Fig. 7. The residual stress of the (100) film was much higher than that of the (111) film (143 MPa and 85.8 MPa, respectively). The film with the small grain size had a higher residual tensile stress [20]. The grain size is one of the most significant factors determining the residual stress. Consequently, it affects the electrical properties of the films. The microstructural characteristics of the film as a result of the grain size and orientation simultaneously affect the electrical properties.

4 Conclusions

The PZT films fabricated using PZT(60/40) targets with various amounts of excess PbO showed differences in microstructural evolution. The Pb content in the film played an important role in the pyrochlore-to-perovskite transformation as well as the nucleation and growth behavior, which in turn significantly affected their preferred orientation, microstructure and susceptibility to crack generation.

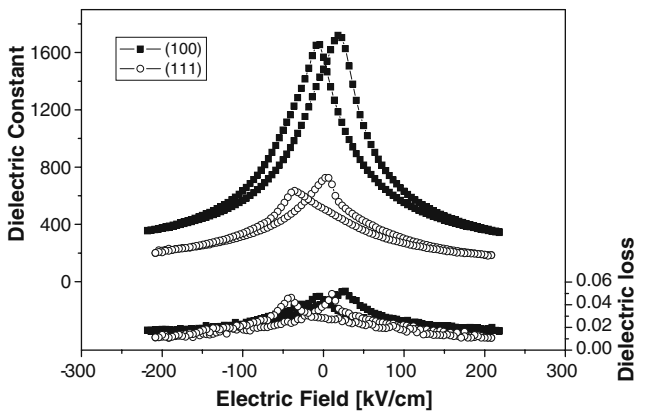

Fig. 5 Dielectric properties of the (100) and (111) oriented films

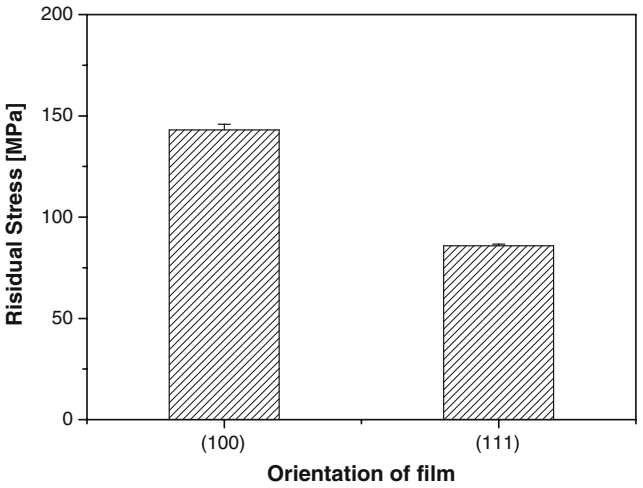

Fig. 7 Residual stress of the (100) and (111) oriented films

(100) or (111) oriented PZT films with different microstructures without any cracks were deposited from targets with the appropriate Pb content. The (100) and (111) oriented films had significantly different electrical properties. The P_r and E_c values of the (111) film were higher than those of the (100) film. On the other hand, the (100) film showed a better dielectric constant and piezoelectric constant than the (111) film. These electrical properties were found to depend strongly on the microstructural characteristics and orientation of the films.

Reference

1. N. Setter, D. Damjanovic, L. Eng, G. Fox, S. Gevorgian, S. Hong, A. Kingon, H. Kohlstedt, N.Y. Park, G.B. Stephenson, I. Stolitchnov, A.K. Taganstev, D.V. Taylor, T. Yamada, S. Stereiffer, J. Appl, Phys. **100**, 051606–1 (2006)
2. K. Yanakawa, K. Imai, O. Ariumi, T. Arikado, M. Yoshioka, T. Owada, K. Okumura, Jpn. J. Appl. Phys. Part I **41**, 2630 (2002)
3. D.L. Polla, L.F. Francis, MRS Bull. **21**, 59 (1996)
4. S.M. Spearing, Acta Mater. **48**, 179 (2000)
5. R. Thomas, S. Mochizuki, T. Mihara, T. Ishida, Mater. Sci. and Engine. **B95**, 36 (2002)
6. I.M. Reaney, K. Brooks, R. Klissurska, C. Pawlaczyk, N. Setter, J. Am, Ceram. Soc. **77**, 1209 (1994)
7. X. Du, J. Zheng, U. Belegundu, K. Uchino, Appl. Phys. Lett. **72**, 2421 (1998)
8. D.V. Taylor, D. Damjanovic, Appl. Phys. Lett. **76**, 1615 (2000)
9. K.G. Brooks, I.M. Reaney, R. Klissurska, Y. Huang, L. Bursill, N. Setter, J. Mater, Res. **9**, 2540 (1994)
10. S.-Y. Chen, I.-W. Chen, J. Am, Ceram. Soc. **77**, 2332 (1994)
11. S.-Y. Chen, I.-W. Chen, J. Am, Ceram. Soc. **77**, 2337 (1994)
12. S. Hiboux, P. Muralt, J. Euro, Ceram. Soc. **24**, 1593 (2004)
13. G.-T. Park, C.-S. Park, J.-J. Choi, H.-E. Kim, J. Mater, Res. **20**, 882 (2005)
14. C.-S. Park, S.-W. Kim, G.-T. Park, J.-J. Choi, H.-E. Kim, J. Mater. Res. **20**, 243 (2005)
15. G.-T. Park, J.-J. Choi, J. Ryu, H. Fan, H.-E. Kim, Appl. Phys. Lett. **80**, 4606 (2002)
16. S.-M. Ha, D.-H. Kim, H.-H. Park, T.-S. Kim, Thin Solid Films **355–356**, 525 (1999)
17. R. Thomas, S. Mochizuki, T. Mihara, T. Ishida, Mater. Sci. Eng. **B95**, 36 (2002)
18. G.A. Rossetti Jr., L.E. Cross, K. Kushida, Appl. Phys. Lett. **59**, 2524 (1991)
19. J.-W. Lee, C.-S. Park, M. Kim, H.-E. Kim, J. Am, Ceram. Soc. **90**, 1077 (2007)
20. W.D. Nix, Metall. Trans. A **20A**, 2217 (1989)